

A new calibration model for pointing a radio telescope that considers nonlinear errors in the azimuth axis *

De-Qing Kong¹, Song-Gen Wang^{1,2}, Jin-Qing Wang³, Min Wang⁴ and Hong-Bo Zhang¹

¹ National Astronomical Observatories, Chinese Academy of Sciences, Beijing 100012, China; kdq@bao.ac.cn

² College of Mechanical Engineering, Hangzhou Dianzi University, Hangzhou 310018, China

³ Shanghai Astronomical Observatory, Chinese Academy of Sciences, Shanghai 200030, China

⁴ Yunnan Observatories, Chinese Academy of Sciences, Kunming 650011, China

Received 2013 October 17; accepted 2014 January 8

Abstract A new calibration model of a radio telescope that includes pointing error is presented, which considers nonlinear errors in the azimuth axis. For a large radio telescope, in particular for a telescope with a turntable, it is difficult to correct pointing errors using a traditional linear calibration model, because errors produced by the wheel-on-rail or center bearing structures are generally nonlinear. Fourier expansion is made for the oblique error and parameters describing the inclination direction along the azimuth axis based on the linear calibration model, and a new calibration model for pointing is derived. The new pointing model is applied to the 40 m radio telescope administered by Yunnan Observatories, which is a telescope that uses a turntable. The results show that this model can significantly reduce the residual systematic errors due to nonlinearity in the azimuth axis compared with the linear model.

Key words: telescopes — antennas — pointing models

1 INTRODUCTION

Pointing accuracy is one of the most important indicators for the performance of radio telescopes, especially radio telescopes with a large diameter or which operate at high frequencies. The general requirement for deviation in pointing is less than 10% of the antenna's half-power beamwidth (Levy 1996).

In general, a new radio telescope with a large aperture cannot point toward a radio source by only using calibrations of the structure that were done during construction, because there are many systematic errors such as axial error, basic plane error and so on. Estimating the pointing calibration of the system via software is the first step to using the telescope. Quite a few engineers introduced the principle and method of acquiring a pointing calibration of a telescope (Meeks et al. 1968; Yuan et al. 1986; Himwich 1993). A linear calibration model is applied in the software that calculates the pointing calibration of most large radio telescopes (Zhang et al. 2009; Meeks et al. 1968; Yuan et al. 1986). Based on pointing measurements using radio sources whose precise locations are known, the pointing errors of the whole sky area are obtained, and the model parameters are identified

* Supported by the National Natural Science Foundation of China.

by using the method of least squares. After predicting deviations in the pointing from this model, the calibrated angles are obtained. However, the linear model does not take nonlinear errors of the structure into considerations. For large radio telescopes, in particular for telescopes with a turntable, because of their massive size and the associated non-uniform precision, it is difficult to correct the pointing errors using a traditional linear calibration model. Nonlinear errors are produced by the wheel-on-rail or center bearing structures. The pointing models based on least-squares support vector machines and generalized interpolation can partly calibrate the pointing error caused by nonlinearity in the structure (Zhao 2008; Kong et al. 2008; Zhang et al. 2007). However, these methods require uniformity in the density of points being measured, and the calibration error might sharply rise in areas where measured points are sparse.

A new model for pointing calibration is deduced on the basis of the linear model by considering the nonlinear error in the azimuth axis. The new pointing model is applied to the 40 m radio telescope administered by Yunnan Observatories, which uses a turntable. The results show that this model can significantly reduce the residual systematic errors due to nonlinearity in the azimuth axis compared with the linear model, and a higher pointing accuracy can be obtained.

Section 2 describes the linear model for pointing calibration. Section 3 describes a pointing calibration model that considers errors from the nonlinear tilt in the azimuth axis. In Section 4, the new pointing model is applied to the 40 m radio telescope administered by Yunnan Observatories. Discussion is presented in Section 5.

2 A LINEAR MODEL FOR POINTING CALIBRATION

The deviation in pointing can be decomposed into two dimensions, the antenna's azimuth and elevation. Pointing accuracy δ (RMS) of the antenna can be expressed as

$$\delta = \left\{ \sum (\delta A_i^2 \cos^2 E_i + \delta E_i^2) / (n - 1) \right\}^{1/2}, \quad (1)$$

where δA_i is the azimuth deviation of the i -th observation point, δE_i is the elevation deviation of the i -th observation point, E_i is the antenna elevation of the i -th observation point and n is the number of observations.

The deviation in pointing of the telescope can be decomposed into azimuth-axis tilt error, the vertical error between the azimuth axis and the elevation axis, the collimation error (the axis of the antenna beam is not exactly perpendicular to the elevation axis), the azimuth and elevation-axis coding zero-error, gravitational deflection error, etc. Since the errors are relatively small, the final pointing deviation is the algebraic sum of all these partial deviations in the linear calibration model. The widely used pointing calibration models are constructed as (Zhang et al. 2009)

$$\begin{cases} \delta A_l = C_1 - C_3 \tan E \cos A \cos(C_4) - C_3 \tan E \sin A \sin(C_4) + C_5 \tan E - C_6 \sec E, \\ \delta E_l = C_2 + C_3 \sin A \cos(C_4) - C_3 \cos A \sin(C_4) + C_7 \cos E + C_8 / \tan E, \end{cases} \quad (2)$$

where δA_l and δE_l are the azimuth and elevation calibration functions, C_1 is the azimuth-axis coding zero-error, C_2 is the elevation-axis coding zero-error, C_3 is the azimuth-axis tilt error, $(\frac{\pi}{2} - C_4)$ is the angle toward which the azimuth axis is tilted, $(\frac{\pi}{2} - C_5)$ is the elongation between the azimuth axis and the elevation axis, C_6 is the collimation error, C_7 is the gravitational deflection error and C_8 is the residual error due to atmospheric correction.

However, nonlinear error is partially ignored in the linear model used for pointing calibration. The error sources associated with a large radio telescope are complicated, and it is difficult to describe all of the pointing errors by the above function, which limits the improvement in pointing accuracy (Zhang et al. 2007).

3 A POINTING CALIBRATION MODEL THAT CONSIDERS ERRORS FROM THE NONLINEAR TILT IN THE AZIMUTH AXIS

The tilt direction of the azimuth axis and tilt error are regarded as the same in the entire azimuth angle in the linear model used for pointing calibration shown in Equation (2). However, the diameter of the track for a radio telescope that has a wheel-on-rail structure is usually up to tens of meters. It is difficult to ensure this quantity has uniform response under high load conditions. For a telescope with a turntable, because the diameter of the turntable is much smaller than the antenna’s aperture, a small error will cause a large pointing error. Therefore, it is necessary to establish a model of the pointing calibration by considering nonlinear errors in the azimuth axis.

Suppose $C_3(A)$ is the tilt error in the azimuth axis and $C_4(A)$ is the inclination direction, which are both functions of azimuth. Considering that the nonlinear errors in the azimuth axis can be expanded into a first-order Fourier series, we obtain

$$\begin{cases} C_3(A) = a_0 + a_1 \sin A + a_2 \cos A, \\ C_4(A) = k_0 + k_1 \sin A + k_2 \cos A, \end{cases} \quad (3)$$

where A is the azimuth, and a_0, a_1, a_2, k_0, k_1 and k_2 are Fourier coefficients.

Substituting Equation (3) into the cosine term in the pointing error caused by tilt in the azimuth axis, $C_3(A) \cos [C_4(A)]$, we obtain

$$C_3(A) \cos [C_4(A)] = [a_0 + a_1 \sin A + a_2 \cos A] \left\{ \cos(k_0) \cos [f_k(A)] - \sin(k_0) \sin [f_k(A)] \right\}.$$

Here $f_k(A) = k_1 \sin A + k_2 \cos A$. Because the second item in the Fourier series is relatively small, the above equation can be approximated as

$$C_3(A) \cos [C_4(A)] \approx [a_0 + a_1 \sin A + a_2 \cos A] \left\{ \cos(k_0) - f_k(A) \sin(k_0) \right\}.$$

Expanding the above equation, the cosine term in the pointing error caused by tilt in the azimuth axis can be expressed as

$$C_3(A) \cos [C_4(A)] = m_0 + m_1 \sin A + m_2 \cos A + m_3 \sin A \cos A + m_4 \cos^2 A, \quad (4)$$

where

$$\begin{aligned} m_0 &= a_0 \cos k_0 - a_1 k_1 \sin k_0, \\ m_1 &= a_1 \cos k_0 - a_0 k_1 \sin k_0, \\ m_2 &= a_2 \cos k_0 - a_0 k_2 \sin k_0, \\ m_3 &= -\sin k_0 (a_1 k_2 + a_2 k_1), \\ m_4 &= -\sin k_0 (a_2 k_2 - a_1 k_1). \end{aligned}$$

Similarly, the sine term in the pointing error caused by tilt in the azimuth axis can be expressed as

$$C_3(A) \sin [C_4(A)] = n_0 + n_1 \sin A + n_2 \cos A + n_3 \sin A \cos A + n_4 \cos^2 A, \quad (5)$$

where

$$\begin{aligned} n_0 &= a_0 \sin k_0 + a_1 k_1 \cos k_0, \\ n_1 &= a_1 \sin k_0 + a_0 k_1 \cos k_0, \\ n_2 &= a_2 \sin k_0 + a_0 k_2 \cos k_0, \\ n_3 &= \cos k_0 (a_1 k_2 + a_2 k_1), \\ n_4 &= \cos k_0 (a_2 k_2 - a_1 k_1). \end{aligned}$$

We assume that pointing errors in the azimuth and elevation directions caused by tilt in the azimuth-axis are denoted $f_A(A)$ and $f_E(A)$, and can be expressed as

$$f_A(A) = -C_3 \cos C_4 \tan E \cos A - C_3 \sin C_4 \tan E \sin A, \quad (6)$$

$$f_E(A) = C_3 \cos C_4 \sin A - C_3 \sin C_4 \cos A. \quad (7)$$

Inserting Equation (4) and Equation (5) into Equation (6), $f_A(A)$ can be expressed as

$$f_A(A) = -\frac{1}{2} \tan E \left[\begin{array}{l} (n_1 + m_2) + (2m_0 + m_4 + n_3) \cos A + (2n_0 + m_3 + n_4) \sin A \\ + (m_2 - n_1) \cos(2A) + (m_1 + n_2) \sin(2A) \\ + (m_4 - n_3) \cos A \cos(2A) + (m_3 + n_4) \sin A \cos(2A) \end{array} \right]. \quad (8)$$

Similarly, $f_E(A)$ can be expressed as

$$f_E(A) = \frac{1}{2} \left[\begin{array}{l} (m_1 - n_2) + (2m_0 + m_4 - n_3) \sin A + (m_3 - 2n_0 - n_4) \cos A \\ + (m_2 - n_1) \sin(2A) - (m_1 + n_2) \cos(2A) \\ + (m_4 - n_3) \sin A \cos(2A) - (m_3 + n_4) \cos A \cos(2A) \end{array} \right]. \quad (9)$$

Inserting Equation (8) and Equation (9) into Equation (2), the pointing calibration model that considers nonlinear error in the azimuth axis can be expressed as

$$\begin{cases} \delta A_n = p_1 + p_2 \tan E \cos A + p_3 \tan E \sin A + p_4 \tan E \cos(2A) + p_5 \tan E \sin(2A) \\ \quad + p_6 \tan E \cos A \cos(2A) + p_7 \tan E \sin A \cos(2A) + p_8 \tan E + p_9 \sec E \\ \delta E_n = p_{10} + p_{11} \cos A + p_{12} \sin A + p_5 \cos(2A) - p_4 \sin(2A) + p_7 \cos A \cos(2A) \\ \quad - p_6 \sin A \cos(2A) + p_{13} \cos E + p_{14} / \tan E \end{cases} \quad (10)$$

where δA_n and δE_n are calibration functions for the azimuth and elevation that arise from nonlinear error in the azimuth axis, and

$$\begin{aligned} p_1 &= C_1, \quad p_2 = -\frac{1}{2} (2m_0 + m_4 + n_3), \quad p_3 = -\frac{1}{2} (2n_0 + m_3 + n_4), \quad p_4 = -\frac{1}{2} (m_2 - n_1), \\ p_5 &= -\frac{1}{2} (m_1 + n_2), \quad p_6 = -\frac{1}{2} (m_4 - n_3), \quad p_7 = -\frac{1}{2} (m_3 + n_4), \quad p_8 = \frac{1}{2} (2C_5 - n_1 - m_2), \\ p_9 &= -C_6, \quad p_{10} = C_2 + \frac{1}{2} (m_1 - n_2), \quad p_{11} = \frac{1}{2} (m_3 - 2n_0 - n_4), \quad p_{12} = \frac{1}{2} (2m_0 + m_4 - n_3) \end{aligned}$$

and

$$p_{13} = C_7, \quad p_{14} = C_8.$$

From Equation (10), it can be seen that it is not necessary to identify the parameters such as $C_1 \sim C_8$, $a_0 \sim a_2$ and $k_0 \sim k_2$. In reality, because each parameter is uncorrelated, the parameters $p_1 \sim p_{14}$ in Equation (10) can be identified by the least squares method and directly applied to the model for pointing calibration.

4 THE POINTING CALIBRATION OF THE 40 m RADIO TELESCOPE ADMINISTERED BY YUNNAN OBSERVATORY

The new pointing model was applied to the 40 m radio telescope in Feb. 2013, which uses a turntable and is administered by Yunnan Observatories. Figure 1 shows a photograph of the 40 m radio telescope. Sources used for calibration observations have strong intensity, small angular diameter and uniform distribution in the sky. The observations were taken in the X-band.

Table 1 lists the main sources we used. In total, 299 positions, which have an almost uniform distribution in the sky, were observed. Table 1 only lists the main sources. The positions were observed for a long time, more than 20 d.



Fig. 1 The 40 m Radio Telescope.

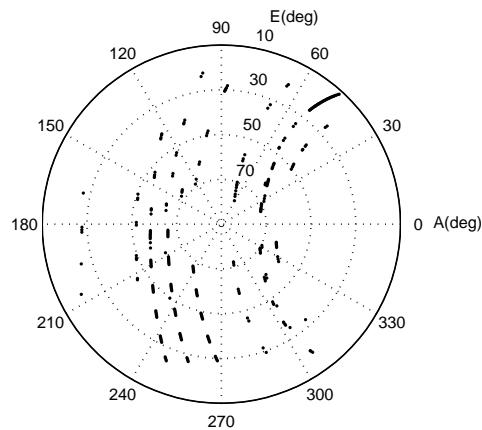


Fig. 2 The sky coverage of observations used in the pointing calibration.

Figure 2 gives the sky coverage. The main parameters associated with the 40 m antenna are that the efficiency of X-band is 0.4, the system noise temperature is 90 K, the bandwidth is 1 GHz and the integration time is 0.1 s. The pointing errors are measured by fitting a Gaussian curve to the scanning data. The observational error of each point caused by noise in the system is less than $1''$ according to the calculation of signal to noise ratio (SNR) for each source.

Results of the pointing calibration for the 4 m radio telescope are shown in Table 2, where e_1 is the error before calibration, e_2 is the residual pointing error after calibration using the linear model for pointing calibration (Eq. (2)) which does not consider nonlinearity in the azimuth axis, and e_3 is the residual pointing error after applying the calibration model (Eq. (10)) which includes nonlinearity in the azimuth axis. It can be seen from Table 2 that the pointing calibration model that includes the nonlinear tilt error from the azimuth axis is significantly better than the linear model, and the accuracy of pointing for the azimuth and elevation axes is largely improved. In particular, the accuracy of points for the azimuth axis increases from $26.6''$ to $9.4''$ which improves by 64.7%. The overall pointing accuracy increases from $33.5''$ to $18.9''$ which improves by 43.6%.

Table 1 The Main Sources Used for the Pointing Calibration

Source name	R.A. (2000)	Dec. (2000)	Type/size('')	Flux (Jy, X-band)
3C84	03 19 48.16	41 30 42.1	Gal./<20	40.0
3C123	04 37 04.17	29 40 15.1	Gal./20	12.0
3C147	05 42 36.14	49 51 07.2	QSO/<1.0	6.0
3C273B	12 29 06.70	02 03 08.6	QSO/<20	40.0
3C279	12 56 11.17	-05 47 21.5	QSO/<2.0	13.0
3C286	13 31 08.29	30 30 33.0	QSO/<2.0	6.0
3C380	18 29 31.72	48 44 47.0	QSO/<2.0	5.0
DR21	05 55 30.81	39 48 49.2	QSO/<10	20.0

Table 2 Comparison of the Pointing Residuals (RMS) of the 40 m Telescope

Item	e_1 ('')	e_2 ('')	e_3 ('')
Azimuth	151.5	26.6	9.4
Elevation	34.1	20.3	16.4
Total	155.3	33.5	18.9

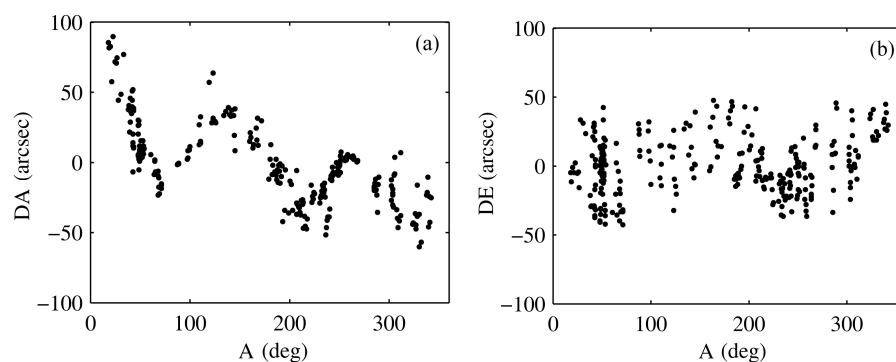
**Fig. 3** The distribution of pointing errors varying with azimuth after applying the pointing calibration using the linear model for calibration (Eq.(2)). (a) Azimuth, (b) Elevation.

Figure 3 shows how the distribution of pointing errors for azimuth and elevation varies with the azimuth after the pointing calibration using the linear calibration model (Eq. (2)) is implemented. It can be seen that there are very significant systematic errors in the residuals, especially the errors in the azimuth, which indicate that there are significant nonlinear errors in the azimuth axis.

Figure 4 shows how the distribution of pointing errors for the azimuth and elevation varies with the azimuth after the pointing calibration is applied using the calibration model (Eq. (10)) that considers nonlinear error in tilt for the azimuth axis. Obviously there are very small systematic errors in Figure 4.

Figure 5 shows the distribution of residual errors in the pointing calibration based on the two calibration models, Equations (2) and (10). As shown, the latter's residual errors obviously decrease, and are basically distributed within $30''$ of the center of the origin.

Figure 6 shows the calibration surfaces of the calibration model considering error in the nonlinear tilt of the azimuth axis.

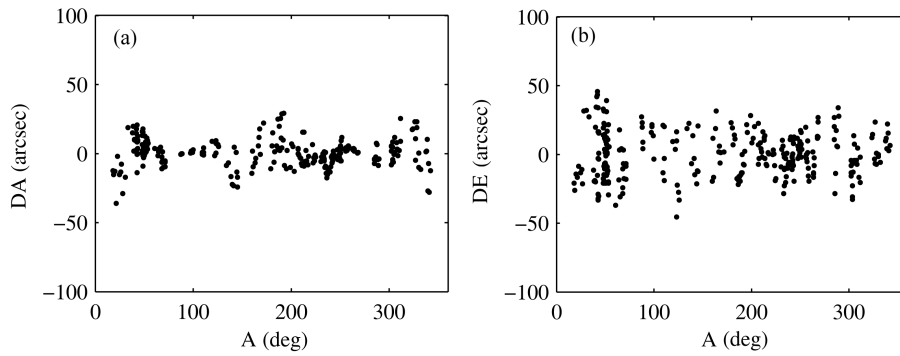


Fig. 4 The distribution of pointing errors varying with azimuth after applying the pointing calibration using the calibration model (Eq. (10)) that considers the nonlinear error in tilt from the azimuth axis. (a) Azimuth, (b) Elevation.

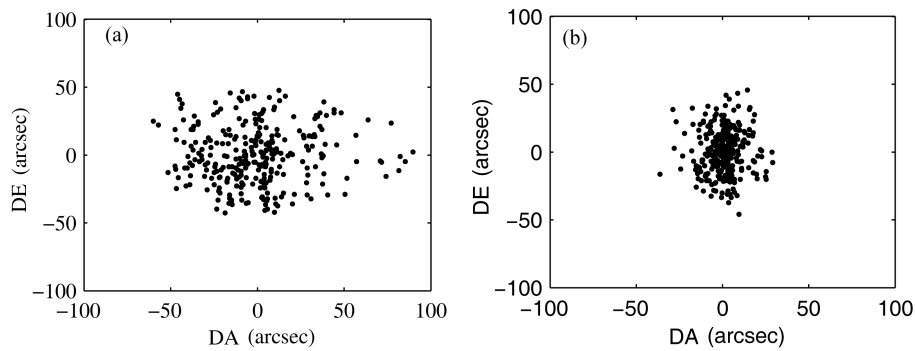


Fig. 5 The distribution of pointing calibration residuals. (a) The linear calibration model (Eq. (2)), (b) The calibration model (Eq. (10)) that considers nonlinear error in tilt from the azimuth axis.

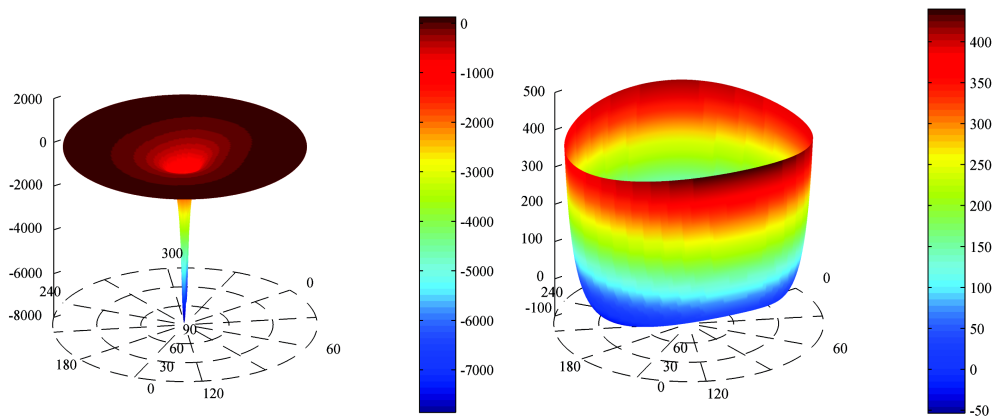


Fig. 6 The calibration surfaces of the calibration model that considers nonlinear error in tilt from the azimuth axis. Azimuth (*left*) and Elevation (*right*).

5 DISCUSSION

The error model for pointing calibration of a radio telescope that considers the nonlinear error in the azimuth axis is presented and is applied to the pointing calibration of the 40 m radio telescope administered by Yunnan Observatories. The results show that this model can significantly reduce the residual systematic errors due to nonlinearity in the azimuth axis compared with the linear model, and a higher pointing accuracy is obtained. The pointing accuracy increases by 43.6% compared with the linear model.

In subsequent work, we will measure vertical errors in the azimuth-axis of the 40 m telescope, and carry out research on the model describing pointing calibration based on measured data. Meanwhile, it can be seen that the residual pointing error in elevation is significantly higher than in azimuth, which is possibly caused by temperature, wind, inaccuracies in the gravity model or other factors, and will also be studied in the the future.

Acknowledgements We thank the National Natural Science Foundation of China (Grant Nos. 10903016 and 11078011) for funding this work. We also thank the operators of the 40 m radio telescope for their assistance in pointing observations.

References

- Himwich, W. E. 1993, Operation Manual of VLBI Mark IV Field System
- Kong, D. Q., Shi, H. L., Zhang, X. Z., & Zhang, H. B. 2008, Journal of Xidian University, 35, 157
- Levy, R. 1996, Structural Engineering of Microwave Antennas for Electrical, Mechanical, and Civil Engineers (Piscataway, NJ: IEEE Press)
- Meeks, M. L., Ball, J. A., & Hull, A. B. 1968, IEEE Transactions on Antennas and Propagation, 16, 746
- Yuan, H. R., Peng, Y. L., & Xue, Y. Z. 1986, Antenna Parameter Measurement Using Radio Astronomical Technique, 147
- Zhang, J. Y., Shi, H. L., Wang, W., & Chen, Z. P. 2007, Chinese Journal of Radio Science, 22, 804
- Zhang, X.-Z., Zhu, X.-Y., Kong, D.-Q., et al. 2009, RAA (Research in Astronomy and Astrophysics), 9, 367
- Zhao, Y. 2008, Research on Modeling Analysis and Design of Pointing Errors for Large Radio Telescope, Ph.D. Thesis (Xian: Xidian Univ.)